

Giant anti-Stokes photoluminescence from semimagnetic heterostructures

Wolfram Heimbrodt

Philipps-University Marburg, Department of Physics and Material Science Center, Renthof 5, D-35032 Marburg, Germany

Michael Happ and Fritz Henneberger

Humboldt-University of Berlin, Institute of Physics, Invalidenstrasse 110, D-10115 Berlin, Germany

(Received 13 October 1999)

A giant anti-Stokes photoluminescence is observed at low excitation densities on specially designed semi-magnetic II–VI asymmetric double quantum well structures by applying an external magnetic field. The signal is due to a two-step absorption process, mediated by a long-living spatially indirect exciton, created via rapid electron tunneling from the primarily excited direct exciton state. [S0163-1829(99)52748-3]

Anti-Stokes photoluminescence (ASPL) is a phenomenon in which the photon energy of the emission is larger than the one of excitation. It has been observed on various systems as molecules, isolators, semiconductors, and quantum wells.^{1–13} However, the efficiency is generally very low at practical excitation levels. In this article we report on a giantly enhanced ASPL signal, occurring in a specially designed semi-magnetic heterostructure. Applying an external magnetic field, the s,p-d exchange interaction between carriers and magnetic ions enables us to tune the band offsets in a desired way. Our study is based on an asymmetric double quantum well (ADQW) structure. Conversely to standard tunneling experiments,^{14,15} excitation of the well with lower optical transition energy gives rise to strong emission from the second well at higher photon energy. By applying an external magnetic field, a band alignment is achieved for which efficient tunneling of the electrons takes place, whereas tunneling of the holes is forbidden.¹⁶ As a result, a spatially indirect or crossed exciton is formed in a first step, with an energy still lower than that of the primarily excited well. Because of the reduced electron-hole overlap, the lifetime of the crossed exciton is substantially increased and, before recombining, it may thus absorb a second photon by an intraband-type transition. The two-step absorption creates electron-hole pairs in the energy continuum of the ADQW structure, which subsequently relax back towards the well states, where they give rise to emission from both wells with almost equal magnitude.

The ADQW structure consists of a magnetic $\text{Zn}_{1-x-y}\text{Cd}_x\text{Mn}_y\text{Se}$ well (MW) and a nonmagnetic $\text{Zn}_{1-x}\text{Cd}_x\text{Se}$ well (NMW) ($x=0.15$, $y=0.09$), separated by a ZnSe barrier, all of 6 nm thickness. The structure is on top of 1 μm ZnSe buffer layer, grown on (100) GaAs substrate, and capped by 20 nm ZnSe. A cw dye laser is used for optical excitation. Fig. 1(a) depicts photo-luminescence (PL) spectra for various excitation densities at a magnetic field of $B=7.5\text{T}$. The laser photon energy is resonant on the heavy-hole (HH) exciton PL excitation peak of the MW (see Fig. 2) and hence distinctly energetically below the optical transitions of the NMW. The PL of the MW is low-energy shifted due to localization on alloy disorder. The striking feature is, however, the occurrence of ASPL from the NMW on the high-energy side, already for excitation densities as low as

$40 \mu\text{W}/\text{cm}^2$. At $2 \text{ W}/\text{cm}^2$, both PL signals are of the same order of magnitude. The spectral details of the ASPL are of minor importance in the present context. We thus merely note that, in addition to the HH band, there is a low-energy contribution, which increasingly dominates the signal at higher excitation levels. This behavior is consistent with bi-exciton emission, as previously observed on (Zn,Cd)Se/ZnSe single quantum well structures.^{17,18} On the Stokes side in Fig. 1(a) along with the HH-PL of the MW, a further PL band is observed exhibiting a significant high-energy shift with increasing excitation density. In what follows we argue that this feature is associated with a spatially indirect exciton state of the ADQW.

Fig. 1(b) summarizes PL spectra for various magnetic-field strengths. The excitation is here above the ZnSe barrier. The PL of the NMW undergoes virtually no shift up to 7.5 T. The feature located at low fields on the high-energy side is due to the spatially direct MW exciton. This band exhibits a strong shift to lower energies and crosses the NMW exciton state. Parallel, at about $B=1.5\text{T}$, the indirect exciton PL appears. Its magnetic-field shift is markedly smaller than that of the direct MW exciton. This is even more clearly seen in Fig. 2, where the PL excitation peaks of the HH-MW and HH-NMW as well as the PL of the indirect exciton are plotted versus magnetic field. The reduced shift represents direct evidence for the fact that only one of the exciton constituents—namely the hole as demonstrated by the subsequent quantitative analysis—is experiencing coupling with the Mn ions. The exciton energies of the ADQW can be written as

$$E_X^{I,J} = E_G^{I,J} + E_h^I + E_e^J + E_b^{I,J} \quad (I, J = \text{MW, NMW}), \quad (1)$$

where the superscripts refer to states with the electron and hole dominantly localized in well I and J , respectively. The zero-field bandgaps E_G of the NMW (2.616 eV) and MW (2.644 eV) were determined on reference epilayers with the same composition. The strain contributions for the ADQW are included in the same way as in Ref. [16]. The single-particle confinement energies E_e and E_h are calculated by means of the transfer matrix method in envelope function

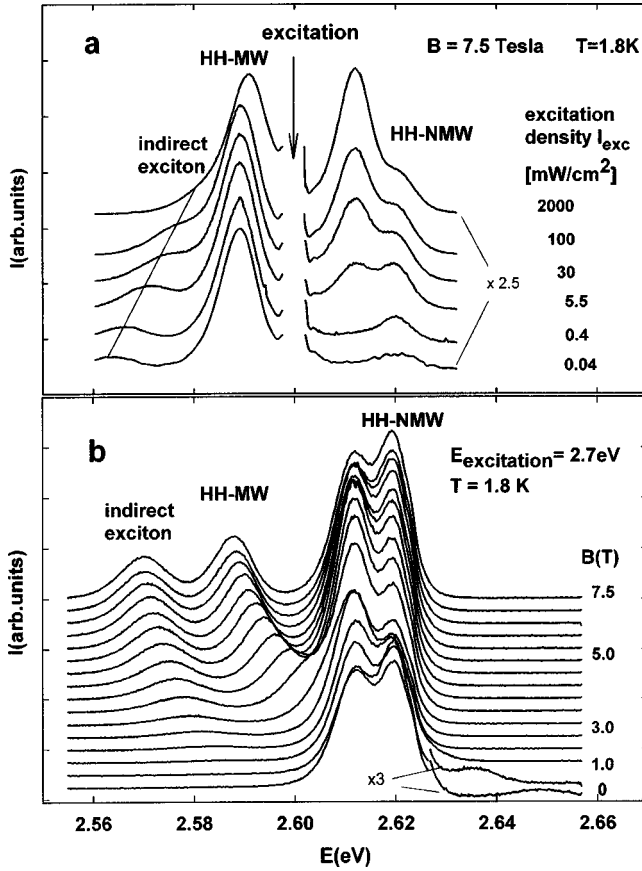


FIG. 1. (a) Stokes and anti-Stokes PL spectra of a semimagnetic ADQW structure at various excitation densities. (b) PL spectra at various magnetic field strengths for an excitation energy above the ZnSe barrier.

approximation and the exciton binding energies E_b using an approach forwarded in Ref. 19. The key role in our study is played by the s,p-d exchange interaction, accounted for by adding the terms

$$H_{ex}^{(p)} = y_{\text{eff}} N_0 J_p \sigma_z \langle S_z \rangle \quad (2)$$

to the band-structure Hamiltonian of the MW. Here, $y_{\text{eff}} = \alpha y$ is the effective Mn concentration, $N_0 J_p$ is the exchange integral for the conduction ($p=e$) and valence band ($p=hh$), σ_z is the carrier spin, and $\langle S_z \rangle$ is the thermal average of the Mn spin system, given in mean-field approximation by

$$\langle S_z \rangle = -\frac{5}{2} B_{5/2}(\zeta); \zeta = \frac{5 \mu_B B}{k_B (T + \Theta)} \quad (3)$$

with the Brillouin function $B_{5/2}$. By phenomenologically introducing the parameters θ and α , clustering of the magnetic ions, Mn-Mn superexchange as well as interface effects are taken into consideration. A nonideal interface is known to enhance the magnetic behavior.^{20,21} Directly induced field variations, present also for the energy states of the nonmagnetic layers, can be ignored in comparison with the much stronger influence of the s,p-d exchange interaction. From the relevant parameters, the band masses ($m_e = 0.143$, $m_{hh} = 0.75$), exchange integrals ($N_0 J_e = 0.26$ eV, $N_0 J_{hh} = -1.31$ eV) and the relative valence band offset (30%) for the

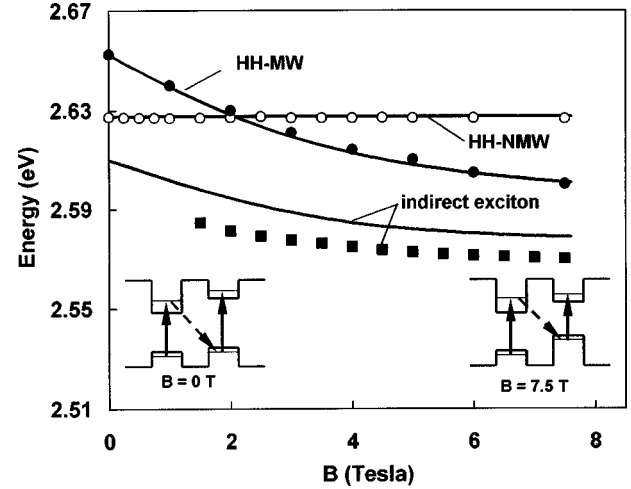
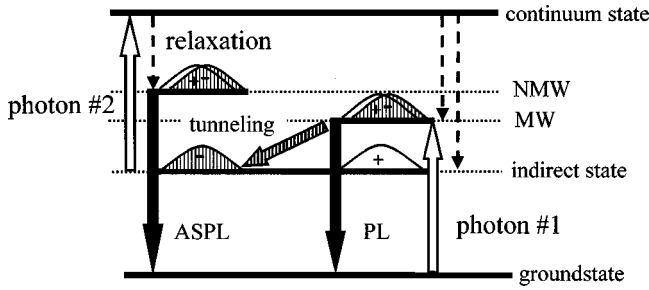


FIG. 2. Exciton energies of the ADQW versus magnetic field strength. Points are experimental data: PL excitation bands for HH-MW and HH-NMW, but PL for the crossed exciton. Curves are calculated exciton energies. For the crossed exciton, a localization-induced PL shift of 10 meV is estimated from the 15 meV line-width. Inset: band alignments of the ADQW at low and high magnetic fields.

(Zn,Cd)Se/ZnSe heterointerface are available from literature data.^{22,23} Excellent agreement between the experimental line positions and the calculated exciton energies, likewise plotted versus magnetic field in Fig. 2, is obtained with $\alpha = 0.31$, $\Theta = 2.6$ K, and a relative (Zn,Cd,Mn)Se/ZnSe valence band offset of 60%. In principle, the crossed exciton provides very direct access to the latter quantity. However, the absence of this state in absorption due to its low oscillator strength—in the fit of Fig. 2 we have postulated a 10 meV low-energy PL shift—makes the deduced value still somewhat uncertain. Despite this, the data reveal unambiguously a type-II band alignment of the ADQW, so that the indirect exciton with electron in the NMW and hole in the MW is indeed the state of lowest energy. This conclusion would be also valid for a much smaller or even reversed zero-field valence band offset between the NMW and MW, since the exchange coupling of the holes is by far dominant ($N_0 J_{hh} \approx 5 N_0 J_e$).

A further difference between the three exciton states concerns their excitation-intensity dependence [Fig. 1(a)]. There is no measurable shift of the NMW exciton PL band. The slight high-energy shift of the HH-MW feature is consistent with heating of the Mn spin system via spin-spin scattering or energy transfer to internal $\text{Mn}^{2+}(3d^5)$ transitions, both reducing the effective momentum $\langle S_z \rangle$ and by this the low-energy shift caused by the exchange interaction. Those effects can, however, not account for the much larger high-energy shift of the crossed exciton. This strong intensity-dependence is a characteristic feature of the spatially indirect state, associated with built-up of an electric field, when electrons and holes populate different wells. The energy change of the direct exciton transitions induced by this field is $\Delta E_{\text{dir}} \approx \pm (4 \pi e^2 n_{\text{id}} / 2 \epsilon) \int dz z^2 [\varphi_e^2(z) - \varphi_h^2(z)]$, where φ_i^2 ($i=e,h$) denotes the respective single-particle probability distribution and n_{id} the crossed exciton density. It is hence much smaller than that of the indirect state, which perceives the total voltage drop across the ADQW. Ignoring for a


 FIG. 3. Scenario of the ASPL formation ($B > 4$ T).

rough estimate any wavefunction penetration into the barriers ($\Delta E_{\text{dir}} = 0$), one readily obtains $\Delta E_{\text{ind}} = 23.4e^2 n_{\text{ind}} d^2 \epsilon$. For the present layer thicknesses of $d = 6$ nm, densities in the 10^{17} cm^{-3} range are required to reproduce the experimentally observed shift. In view of the long lifetime, this density is in accordance with the low excitation levels in Fig. 1(a).

After having clarified the energy structure of the semimagnetic ADQW, we return to the mechanism of the huge ASPL signal. The scenario described already in the introduction is again depicted schematically in Fig. 3. We emphasize that the ASPL occurs only beyond the magnetically induced crossover of the direct exciton states. At lower magnetic fields, tunneling of the hole from the NMW into the MW is required. The energy separation between initial and final state is here, however, clearly below the 1-LO-phonon threshold of $\hbar\omega_{\text{LO}} \approx 30$ meV (see Fig. 2). In conjunction with the heavier hole mass, this results in acoustic-phonon mediated tunneling times of several 100 ps,²⁴ excluding this process in view of the shorter direct exciton lifetime (see below). In this way, the general requirement for efficient ASPL, that carriers do not relax back to the low-bandgap material before radiatively recombining, Ref. 13 is automatically fulfilled. In contrast, tunneling by LO-phonon assistance, as energetically allowed for the MW exciton in the initial state, is typically two orders of magnitudes faster.²⁴

For a direct proof of the two-step absorption process, a second cw laser ($\lambda = 632.8$ nm) was used for independent excitation of the ADQW with a photon energy far below the exciton transitions. The extra light can thus only drive the second intraband-type transition. It is clearly seen in Fig. 4 that additional excitation with low-energy photons increases the ASPL signal, while it leaves the Stokes PL from the MW unchanged. The indirect exciton, being the initial state for the intraband absorption step, is low-energy shifted and reduced in intensity. Both features are entirely consistent with depopulation of the indirect state. Enumeration of the spectrally integrated signal change yields in fact that the gain of the ASPL equals closely the loss of the indirect exciton PL. Our finding is different from related studies on GaAs/(Al, Ga)As heterostructures, where stimulation of the ASPL is solely found for frequencies of the second beam above the GaAs bandgap Ref. 13. The present two-step absorption deviates also from the standard process with photon recycling Refs. 7 and 8, since only one electron-hole pair is required for ASPL generation.

To understand in more detail the parameter constellation behind the strong ASPL, we have analyzed its intensity dependence by using the standard rate equations for the 5-level

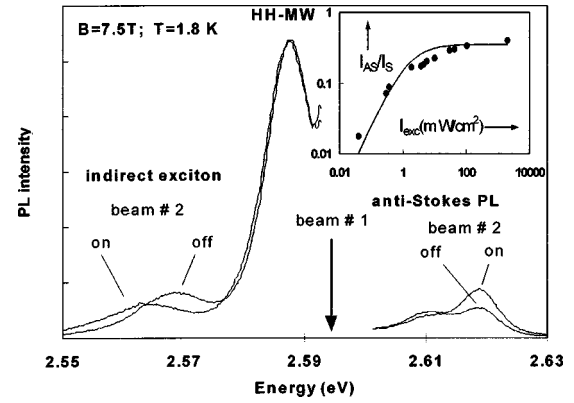


FIG. 4. PL spectra for single-beam ($\hbar\omega_1 = 2.595$ eV) and two-beam excitation ($\hbar\omega_1 = 2.595$ eV; $\hbar\omega_2 = 1.959$ eV). Inset: Ratio of the spectrally integrated anti-Stokes and Stokes signals versus excitation intensity (single beam), symbols: experiment, line: calculation with Eq. (4).

system in Fig. 3. Let β be the cross section for the intraband transition starting from the indirect exciton level (with absorption coefficient $\beta_{\text{ind}} n_{\text{ind}}$). Time-resolved PL measurements have yielded a life-time of $\tau_{\text{NMW}} = 50$ ps and $\tau_{\text{MW}} = 30$ ps at $B = 7.5$ T for the direct NMW and MW exciton, respectively.²⁵ These times are too short for efficient intraband absorption involving the direct states. The indirect exciton lifetime τ_{ind} was not accessible by our 76 MHz repetition ps setup and is therefore at least several 10 ns. It is hence certainly much longer than the time for the relaxation back from the continuum into to the well excitons (assumed to be same for all three states for simplicity). Denoting the electron tunneling time by τ_{T} , we find for the anti-Stokes versus Stokes ratio in steady state

$$\frac{I_{\text{AS}}}{I_{\text{S}}} = \frac{\tau_{\text{MW}}^{(\text{rad})}}{\tau_{\text{NMW}}^{(\text{rad})}} \frac{n_{\text{NMW}}}{n_{\text{MW}}} = \frac{\tau_{\text{NMW}}}{\tau_{\text{NMW}}^{(\text{rad})}} \frac{\tau_{\text{MW}}^{(\text{rad})}}{\tau_{\text{T}}} \frac{I_{\text{exc}}}{3I_{\text{c}} + 2I_{\text{exc}}}, \quad (4)$$

with the characteristic intensity $I_{\text{c}} = \hbar\omega/\beta\tau_{\text{ind}}$. This formula reproduces the experimental curve indeed adequately well (see inset of Fig. 4). Under the reasonable assumption of equal radiative lifetimes $\tau_{\text{NMW}}^{(\text{rad})} \cong \tau_{\text{MW}}^{(\text{rad})}$ for the direct excitons, one obtains $\tau_{\text{T}} = 70$ ps and $I_{\text{c}} = 0.9$ mW/cm² from the fit. The dipole moment of the intraband transition scales like $f \times d$, where the prefactor f depends on the details of the QW wavefunctions. Considering d^2 as an upper limit for β , we find $\tau_{\text{ind}} \geq 0.96$ μs . We recognize that the appearance of the ASPL at these exceedingly low excitation levels is a consequence of the very long indirect exciton lifetime. On the other hand, the yield of the signal is inversely proportional to the tunneling time. Because of the electric-field induced shift of the indirect state, the energy condition for the tunneling changes with optical power and drops eventually below the LO-threshold. The 70 ps time, deduced from the saturation level of $I_{\text{AS}}/I_{\text{S}}$ in Fig. 4, is indeed consistent with acoustic-phonon assisted tunneling of the five times lighter electron. We note therefore that even higher ASPL efficiencies may be achieved by maintaining the LO-process.

In summary, we have reported on giant ASPL from a semimagnetic ADQW structure. The underlying mechanism is a two-step absorption process mediated by a spatially in-

direct exciton. The very low excitation densities ($\mu\text{W}/\text{cm}^2$) required to observe the ASPL make this process an ideal candidate for optical up-conversion. In the present case, the magnetic field was needed for achieving sufficiently fast direct-to-indirect tunneling. Similarly efficient ASPL will occur

in any type-II heterostructure with a parameter design close to the present one.

The authors acknowledge financial support by the Deutsche Forschungsgemeinschaft.

-
- ¹Z. G. Soos and R. G. Kepler, *Phys. Rev. B* **43**, 11 908 (1992).
²S. B. Mirov *et al.*, *J. Lumin.* **69**, 35 (1996).
³S. Q. Gu *et al.*, *Phys. Rev. Lett.* **69**, 2697 (1992).
⁴V. Yu. Ivanov *et al.*, *Phys. Rev. B* **54**, 4696 (1996).
⁵Z. Hasan *et al.*, *Phys. Rev. B* **56**, 4518 (1997).
⁶A. Tomita *et al.*, *Phys. Rev. B* **53**, 10 793 (1996).
⁷R. Hellmann *et al.*, *Phys. Rev. B* **51**, 18 053 (1995).
⁸Young-Hon Cho *et al.*, *Phys. Rev. B* **56**, 4375 (1997).
⁹W. Seidel *et al.*, *Phys. Rev. Lett.* **73**, 2356 (1994).
¹⁰Z. P. Su *et al.*, *Solid State Commun.* **99**, 933 (1996).
¹¹M. Potemski *et al.*, *Phys. Rev. Lett.* **66**, 2239 (1991).
¹²J. Zeman *et al.*, *Phys. Rev. B* **55**, R13 428 (1997).
¹³H. M. Cheong *et al.*, *Phys. Rev. B* **58**, R4254 (1998).
¹⁴I. Lawrence *et al.*, *Phys. Rev. Lett.* **73**, 2131 (1994).
¹⁵K. Hieke *et al.*, *Solid State Commun.* **93**, 257 (1995).
¹⁶W. Heimbrod *et al.*, *Phys. Rev. B* **58**, 1162 (1998).
¹⁷F. Kreller *et al.*, *Phys. Rev. Lett.* **75**, 2420 (1995).
¹⁸G. Kuang *et al.*, *Appl. Phys. Lett.* **70**, 2717 (1997).
¹⁹R. P. Leavitt and J. W. Little, *Phys. Rev. B* **42**, 11 774 (1990).
²⁰J. A. Gaj *et al.*, *Phys. Rev. B* **50**, 5512 (1994).
²¹W. Heimbrod *et al.*, *J. Cryst. Growth* **159**, 1005 (1996).
²²A. Twardowski *et al.*, *Solid State Commun.* **51**, 849 (1984).
²³A. Rajira *et al.*, *Solid State Commun.* **105**, 229 (1998).
²⁴S. Ten *et al.*, *Phys. Rev. B* **53**, 12 637 (1996).
²⁵A point that deserves further investigation is the very short lifetime of the MW exciton ($\tau_{\text{MW}}=15$ ps) at low magnetic fields, probably caused by inner Mn transitions. It is the reason why the indirect exciton, though being the lowest energy state, becomes only visible beyond the crossover for ZnSe excitation in Fig. 1(b).